Cellular Signalling 134 (2025) 111929

Contents lists available at ScienceDirect

Cellular Signalling

journal homepage: www.elsevier.com/locate/cellsig

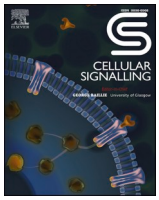

GLCCI1 ameliorates mitochondrial dysfunction in allergic asthma mice via DYRK1A/FAM117B-dependent NRF2 activation

Qiufen Xun *, Qing Yang, Wei Wang, Guofeng Zhu

Department of Respiratory and Critical Care Medicine, Second Affiliated Hospital of Nanchang University, Nanchang 330006, Jiangxi, China

ARTICLE INFO

Keywords:
Allergic asthma
Mitochondrial dysfunction
GLCCI1
NRF2

ABSTRACT

Allergic asthma significantly impacts individuals' quality of life and work. This study aimed to investigate the specific mechanisms by which GLCCI1 regulated mitochondrial dysfunction in allergic asthma mice. In an ovalbumin (OVA)-induced allergic asthma mouse model, mitochondrial dysfunction in airway epithelium was observed, characterized by reduced ATP production, decreased mtDNA copy number, ROS accumulation, and mitophagy activation (upregulated PINK1/OPTN). In vitro experiments confirmed that OVA stimulation impaired mitochondrial membrane potential, exacerbated oxidative stress, and reduced cell viability in bronchial epithelial cells (BECs). Moreover, GLCCI1 regulated DYRK1A/FAM117B and KEAP1/NRF2 axis while inhibiting NRF2 ubiquitination degradation. Mechanistically, GLCCI1 overexpression reversed OVA-induced mitochondrial dysfunction by activating NRF2 signaling pathway via enhancing DYRK1A/FAM117B. In allergic asthma mice, GLCCI1 overexpression improved airway hyperresponsiveness, reduced inflammatory infiltration, restored alveolar structure, and decreased IL-4/IL-5/IL-13 levels. In summary, GLCCI1 ameliorated mitochondrial dysfunction in allergic asthma mice via the DYRK1A/FAM117B/NRF2 pathway, offering a potential therapeutic target for allergic asthma.

1. Introduction

Asthma affects over 330 million individuals globally throughout their educational and professional lives, with exacerbations imposing a significant burden on productivity [1]. Allergic asthma is the most prevalent phenotype of asthma, characterized by sensitization to inhaled allergens that results in asthma symptoms and airway inflammation [2]. The management of allergic asthma encompasses environmental control measures, allergen immunotherapy, and corticosteroids [3]. Given the rapid advancements in immunology, molecular biology, and biotechnology, elucidating the specific pathogenesis of allergic asthma is crucial for the development of novel biological therapies aimed at treating this condition [4].

Studies have indicated that allergic asthma is linked to mitochondrial dysfunction [5,6]. Bronchial epithelial cells (BECs), serving as the primary interface between the body and the environment, are crucial in the context of allergic asthma [7,8]. Mabalirajan et al. have demonstrated that ovalbumin (OVA) leads to mitochondrial dysfunction in BECs of experimental mice with allergic asthma [9]. The loss of nuclear factor erythroid 2-related factor 2 (NRF2) is known to induce mitochondrial dysfunction [10]. Furthermore, research has shown decreased levels of NRF2 in BECs exhibiting mitochondrial dysfunction [11]. In atherosclerotic mice, the activation of the Kelch-like ECH-associated protein 1 (KEAP1)/NRF2 pathway has been found to enhance mitochondrial function and inhibit macrophage ferroptosis [12]. Although these studies confirm the significant role of the NRF2 pathway in mitigating mitochondrial dysfunction, the upstream mechanisms that regulate the NRF2 pathway in allergic asthma remain

Abbreviation: BECs, Bronchial epithelial cells; BCA, bicinchoninic acid; CCK-8, Cell Counting Kit-8 assay; Cdyn, dynamic lung compliance; Cleaved PARP, Cleaved polymerase; Co-IP, Co-immunoprecipitation; DCFH-DA, 2,7-dichlorofluorescein diacetate; DHE, Dihydroethidium; DMEM, Dulbecco's Modified Eagle Medium; DYRK1A, dual-specificity tyrosine phosphorylation-regulated kinase 1 A; ECL, enhanced chemiluminescence; FAM117B, family with sequence similarity 117, member B; GLCCI1, Glucocorticoid Induced 1; GSH/GSSG, glutathione/oxidized glutathione; IF, Immunofluorescence; IHC, Immunohistochemistry; KEAP1, Kelch-like ECH-associated protein 1; mtDNA, mitochondrial DNA; NRF2, nuclear factor erythroid 2-related factor 2; OCR, oxygen consumption rate; OPTN, optineurin; OVA, ovalbumin; PINK1, PTEN-induced putative kinase 1; PVDF, Polyvinylidene fluoride; qRT-PCR, Quantitative Real-time PCR; RL, transpulmonary resistance; ROS, reactive oxygen species; SOD, superoxide dismutase; SPF, Specific Pathogen Free; TFAM, mitochondrial transcription factor A; WB, Western blotting.

* Corresponding author at: No.1 Minde Road, Donghu District, Nanchang 330006, Jiangxi, China.
E-mail address: ndefy17054@ncu.edu.cn (Q. Xun).

https://doi.org/10.1016/j.cellsig.2025.111929
Received 11 February 2025; Received in revised form 30 May 2025; Accepted 6 June 2025
Available online 7 June 2025

unclear.

Glucocorticoid Induced 1 (GLCCI1) is a candidate factor implicated in the regulation of thymic T cell apoptosis [13]. Literature reports indicate that the mRNA expression levels of GLCCI1 and NRF2 in patients with severe asthma are significantly lower than those in patients with non-severe asthma [14]. Previous studies have demonstrated that GLCCI1 mitigates collagen deposition and airway hyperresponsiveness in OVA-induced asthma mouse models [15]. Moreover, overexpression of GLCCI1 has been shown to decrease apoptosis and mitochondrial swelling of retinal ganglion cells in a high glucose environment [16]. However, the relationship between GLCCI1 and mitochondrial dysfunction remains unexplored.

Emerging evidence demonstrates that dual-specificity tyrosine phosphorylation-regulated kinase 1 A (DYRK1A) inhibition induces mitochondrial dysfunction and endoplasmic reticulum stress, thereby promoting autophagic cell death in cancer models [17]. Moreover, DYRK1A overexpression has been shown to activate the NRF2 signaling pathway in murine liver tissues [18]. Notably, a recent study elucidates that family with sequence similarity 117, member B (FAM117B) competitively binds to KEAP1, thereby reducing NRF2 ubiquitination and activating the KEAP1/NRF2 signaling axis [19]. Through comprehensive STRING database analysis, we further identified documented protein-protein interactions between GLCCI1 and DYRK1A [20], as well as between DYRK1A and FAM117B [21]. Consequently, we hypothesized that GLCCI1 might regulate NRF2 through DYRK1A/FAM117B, potentially influencing mitochondrial dysfunction in BECs in allergic asthma models.

This study developed animal and cell models to investigate the specific mechanism by which GLCCI1 impacts the progression of allergic asthma. The results indicated that GLCCI1 alleviated mitochondrial dysfunction in allergic asthma mice by activating the NRF2 pathway through regulation of the DYRK1A/FAM117B axis. These findings offered new insights into the pathogenesis of allergic asthma.

2. Materials and methods

2.1. Animals

The Balb/c mice (aged 6 week) (Spiff Biotechnology Co., LTD, Beijing, China) were housed in the breeding environment of the Specific Pathogen Free (SPF) grade standard, keeping constant temperature (21–23 °C) and constant humidity (60–65 %). The animals were provided with standard laboratory chow and sterile water ad libitum. Following a one-week acclimatization period, all experimental procedures were initiated in accordance with the institutional guidelines approved by the Ethics Committee of Second Affiliated Hospital of Nanchang University.

2.2. Allergic asthma mouse model

Mice were randomly divided into a Control (CON) group and an OVA group. To construct an allergic asthma model, mice were sensitized to OVA through intraperitoneal injection of 0.2 mL of physiological saline solution containing 50 μg of OVA (Macklin, Shanghai, China) and 2 mg of aluminum hydroxide (Biodragon, Suzhou, Jiangsu, China) on days 0, 7, and 14. Between days 21 and 27, OVA-sensitized mice were exposed to aerosolized 5 % OVA using a nebulizer for 30 min once daily. Mice in the CON group received intraperitoneal injections and nebulization with normal saline according to the same schedule but did not receive OVA treatment. To investigate the role of GLCCI1 in allergic asthma mouse models, mice were further divided into the OVA+LV-NC group and the OVA+LV-GLCCI1 group. On day 18 of the OVA sensitization protocol, LV-NC or LV-GLCCI1 lentivirus was administered to mice via intratracheal instillation, while all other procedures for establishing the allergic asthma model were performed as previously described. After assessing the airway hyperresponsiveness of the mice in each group, they were euthanized under anesthesia. Subsequently, lung tissues were collected for further analysis.

2.3. Assessment of airway hyperresponsiveness

Twenty-four hours following model establishment, the airway hyperresponsiveness of mice in each group was quantitatively assessed using the Fine Pointe Resistance and Compliance system (DSI BuxcoElectronics, USA). Briefly, after the trachea of anesthetized mice was incised and intubated, the mice were placed in the chamber and the tracheal tube was connected to the ventilator. Various doses of methacholine (Sigma-Aldrich, Saint Louis, MO, USA) were administered to record the transpulmonary resistance (RL) and dynamic lung compliance (Cdyn) of the mice in each group.

2.4. Hematoxylin eosin (H&E) staining

Lung tissue samples fixed in 4 % paraformaldehyde underwent standard histological processing, including graded ethanol dehydration, xylene clearing, and paraffin embedding. Using a rotary microtome, we obtained 4-μm thick serial sections from intact tissue blocks. After drying, sections were deparaffinized. Following distilled water rinses, tissue sections were successively stained with hematoxylin (Servicebio, Wuhan, Hubei, China) for 5 min and eosin (Servicebio) for 5 s. After being washed with distilled water again, sections were dehydrated and sealed. Subsequently, the staining of the lung tissue was observed with a microscope.

2.5. Cell and culture

The human BECs (BEAS-2B cell line) was purchased from Shanghai Enzyme Research Biotechnology (Shanghai, China). The cells were cultured in Dulbecco's Modified Eagle Medium (DMEM) (Servicebio) containing 10 % fetal bovine serum (Gibco, Waltham, MA, USA) and 1 % penicillin/streptomycin (Solarbio, Beijing, China). Cells were routinely cultured at 37 °C and 5 % CO_2. To simulate BECs in allergic asthma models, BECs cells were incubated with 5 μg/mL OVA for 24 h to establish an OVA-stimulated cell model.

2.6. Cell transfection

BECs were cultured until the number of cells had increased by about 70 %–80 % in 24-well culture plates, and the previous medium of the cultured cells was removed. After washing the cells twice with PBS, the cells were cultured overnight in a new medium. Subsequently, 2 μL of virus at a concentration of 1 × 10^9 PFU/mL was added to each well to transfect BECs. Following a 24-h incubation at 37 °C in 5 % CO_2, the virus-containing culture medium was discarded and replaced with fresh complete culture medium. To investigate the role of GLCCI1 in OVA-stimulated BECs, cells were transfected with various constructs, including NC, GLCCI1-OE, sh-NC, sh-GLCCI1, GLCCI1-OE + sh-NC, GLCCI1-OE + sh-DYRK1A, and GLCCI1-OE + sh-FAM117B, after which OVA stimulation was performed as previously described.

2.7. Cell counting kit-8 (CCK-8) assay

Cell viability of BECs/AECs was evaluated using the CCK-8 assay. Cells were seeded in 96-well plates and allowed to adhere. Following the manufacturer's instructions for the CCK-8 kit (Yeasen, Shanghai, China), 10 μL of CCK-8 solution was added to each well and incubated for an appropriate duration. The absorbance was measured at a wavelength of 450 nm using a microplate analyzer (Thermo Fisher Scientific, Waltham, MA, USA).

2.8. Measurement of oxygen consumption rate (OCR)

OCR was measured using the Seahorse XF Cell Mitochondria Stress Test Kit (Agilent, Santa Clara, CA, USA). BECs were seeded in Seahorse XF24 cell culture plates and incubated overnight in a cell culture incubator maintained at 37 °C with 5 % CO_2. Prior to measuring OCR, the probe card was hydrated using XF Calibration Solution in a CO_2-free incubator. Following the kit's instructions, a detection solution with a pH of 7.4 was prepared, and the OCR of BECs was subsequently measured.

2.9. Determination of reactive oxygen species (ROS) level

Dihydroethidium (DHE) (Beyotime, Shanghai, China) was employed to assess ROS level in lung tissue. Following the manufacturer's instructions, tissue sections were incubated with a 5 μM DHE solution for 30 min at 37 °C. After washing with PBS two times, the fluorescence intensity in the tissue was observed using a fluorescence microscope. The 2,7-dichlorofluorescein diacetate (DCFH-DA) fluorescent probe (Beyotime) was utilized to measure ROS level in BECs. The digested BECs were seeded in a 48-well plate and cultured in a 37 °C incubator for 24 h. After removing the cell culture medium, 200 μL of diluted DCFH-DA was added to each well according to the manufacturer's instructions. Subsequently, the cells were incubated in an incubator at 37 °C with 5 % CO_2 for 30 min. Following three washes with PBS, images were captured and analyzed under a fluorescence microscope.

2.10. Evaluation of mitochondrial membrane potential

Mitochondrial membrane potential was assessed using the JC-1 mitochondrial membrane potential detection kit (Beyotime). JC-1 is a cationic dye that accumulates in mitochondria, forming red fluorescent aggregates in healthy cells but remaining as green fluorescent monomers when membrane potential is decreased. Briefly, cell suspensions of BECs were seeded in 48-well plates and cultured at 37 °C and 5 % CO_2. Subsequently, the JC-1 working solution was prepared according to the manufacturer's instructions to evaluate the mitochondrial membrane potential of BECs subjected to various treatments. Finally, observations and images were captured using a fluorescence microscope.

2.11. Detection of ATP and relevant antioxidant enzymes

ATP content detection kit (Solarbio), superoxide dismutase (SOD) activity assay kit (Solarbio), catalase assay kit (Solarbio) and reduced glutathione/oxidized glutathione (GSH/GSSG) assay kit (Nanjing Jiancheng Bioengineering Institute, Nanjing, China) were used to detect the levels of ATP, SOD, GSH/GSSG in BECs and lung tissues following the manufacturer's instructions.

2.12. Immunohistochemistry (IHC)

After deparaffinization and rehydration, tissue slides were treated with 100 μL endogenous peroxidase blockers for 10 min. Then, the slides were incubated with polyclonal primary antibody against GLCCI1 (A14675, 1:200; Abclonal, Beijing, China), NRF2 (RM8594, 1:200; Biodragon), FAM117B (21768–1-AP, 1:200; Proteintech, Wuhan, Hubei, China), and DYRK1A (PA5–14490, 1:200; Thermo Fisher Scientific) overnight at 4 °C. The tissue slides were treated with Universal IHC kit (PV-6000, Zhongshan Golden Bridge, Beijing, China). Sections were stained with a DAB kit (Servicebio) followed by DAPI. Finally, the protein staining was observed under microscope.

2.13. Immunofluorescence (IF)

BECs were permeated with 0.5 % Trion X-100 for 10 min and closed with 3 % bovine serum albumin (BSA) for 30 min. Then, the cells were incubated with primary antibody against DYRK1A (H00001859-M01, Thermo Fisher Scientific), GLCCI1 (PA5–109769, Thermo Fisher Scientific), FAM117B (21768–1-AP, Proteintech) and KEAP1 (60027–1-Ig, Proteintech) overnight at 4 °C. After rinsing with PBS, sections were incubated with Cy3-conjugated Goat Anti-Mouse IgG (A0521, Beyotime) and FITC-conjugated Goat Anti-Rabbit IgG (A0562, Beyotime) for 1 h at 37 °C away from light. After staining the nucleus with DAPI, the expression and co-localization of DYRK1A/GLCCI1, DYRK1A/FAM117B and FAM117B/KEAP1 were observed by fluorescence microscopy.

2.14. Quantitative real-time PCR (qRT-PCR)

Total RNA was extracted by TRIzol reagent (Invitrogen, Waltham, MA, USA) following the manufacturer's protocol. Total RNA was reversely transcribed into cDNA using PrimeScript RT reagent Kit (Takara, Tokyo, Japan). The expression level of GLCCI1, DYRK1A, and NRF2 in each group was quantified using qRT-PCR kit (Takara), with GAPDH as the internal control. After each reaction was repeated three times, the data were analyzed using $2^{-\Delta\Delta CT}$ method. The primers used in qRT-PCR were listed in Table 1.

2.15. Evaluation of mitochondrial DNA (mtDNA) copy number

PCR was employed to evaluate mtDNA copy number, following the methodology outlined in a previous study [22]. Total DNA was extracted using a mitochondrial DNA extraction kit (Phygene, Fuzhou, Fujian, China). Subsequently, mtDNA quantification was performed using the Mouse Mitochondrial DNA Copy Number Assay Kit (Detroit R&D, Detroit, Michigan, USA). Finally, real time PCR was utilized to measure the mtDNA copy number.

2.16. Western blotting (WB)

RIPA lysis buffer (Thermo Fisher Scientific) was utilized to lyse the tissues or cells. After being detected with a bicinchoninic acid (BCA) kit (Biosharp, Guangzhou, Guangdong, China), the obtained proteins were separated by SDS-PAGE before transferred onto polyvinylidene fluoride (PVDF) membranes (Millipore, Billerica, MA, USA). Membranes were blocked by BSA (5 %) for 1 h at room temperature and then cultured with primary antibodies against GLCCI1 (BD-PB1103, 1:1000; Biodragon), mitochondrial transcription factor A (TFAM) (22586–1-AP, 1:1000; Proteintech), PTEN-induced putative kinase 1 (PINK1) (23274–1-AP, 1:1000; Proteintech), optineurin (OPTN) (10837–1-AP, 1:1000; Proteintech), DYRK1A (ab259869, 1:1000; Abcam, Cambridge, MA, USA), p-DYRK1A (AF3507, 1:1000; Affinity, Golden, CO, USA), FAM117B (21768–1-AP, 1:1000; Proteintech), NRF2 (CY5136, 1:1000; Abways, Beijing, China), Cleaved polymerase (Cleaved PARP) (9541, 1:1000; Cell signaling, Danvers, MA, USA), and β-tubulin (AB0039, 1:1000; Abways) at 4 °C overnight. After washing five times with TBST, the membranes were incubated with HRP-conjugated goat anti-rabbit secondary antibody (ab6721, 1:5000; Abcam) and HRP-conjugated goat anti-mouse secondary antibody (ab6789, 1:5000; Abcam) for 2 h at 37 °C. Finally, we detected the brightness of protein bands using enhanced chemiluminescence (ECL) (Bio-rad, Shanghai, China).

2.17. Co-immunoprecipitation (Co-IP) and ubiquitination analysis

For Co-IP detection, an immunoprecipitation kit utilizing the Protein A + G magnetic bead method (Beyotime) was employed. Protein samples were incubated overnight at 4 °C with antibodies against IgG, DYRK1A, FAM117B, or KEAP1. Following this initial incubation, washed magnetic beads were added to the sample solution and subsequently incubated at 4 °C for an additional 5 h. After five washes with buffer, the precipitated proteins were collected for WB detection. For the analysis of NRF2 ubiquitination, antibodies against NRF2 and Ubiquitin (3936 T, 1:1000; Cell signaling) were used to incubate with the protein

Table 1
Primers of qRT-PCR.

Gene	Forward sequence (5′-3′)	Reverse sequence (5′-3′)
GLCCI1 Human	CGGACCTCTAGTACAATAAGGCG	AGGTGTCTGAGTAGCTTTGTCT
DYRK1A Human	AAGAAGCGAAGACACCAACAG	TTTCGTAACGATCCATCCACTTT
GLCCI1 Mouse	TCAGACACCTAGTTGCTGGG	ACTATGCCGACTACTTTGCTTG
DYRK1A Mouse	GGGGACGATTCCAGTCATAAGA	GGAGTCGATTTCATACCGATCC
NRF2 Human	CACATCCAGTCAGAAACCAGTGG	GGAATGTCTGCGCCAAAAGCTG
GAPDH Human/Mouse	GCACCGTCAAGGCTGAGAAC	TGGTGAAGACGCCAGTGGA

samples, with subsequent assays performed as described above.

2.18. Enzyme-linked immunosorbent assay (ELISA)

ELISA detections were performed according to the instructions of ELISA kits (Elabscience, Wuhan, Hubei, China) including interleukin-4 (IL-4) ELISA kit (*E*-EL-H0101), interleukin-5 (IL-5) ELISA kit (E-EL-H0191), and interleukin-13 (IL-13) ELISA kit (E-EL-H0104).

2.19. Cycloheximide chase assay

To assess the degradation of NRF2, a Cycloheximide chase assay was performed. BECs in Model+NC or Model+GLCCI1-OE groups were treated with ActinomycinD (S8964, Selleck, Houston, TX, USA). Cell lysates were collected at 0, 15, 30, 45, and 60 mins after ActinomycinD treatment. Subsequently, the NRF2 levels in cell lysates obtained at different time periods were detected by WB.

2.20. Statistical analysis

All experiments were performed with three independent biological replicates. Within each biological replicate, triplicate measurements were performed and averaged. Data were analyzed by GraphPad Prism 8.0 (La Jolla, CA, USA) and expressed as mean ± standard deviation. Two-tailed Student's *t*-test were used for comparing two variables. One-way ANOVA test was used for multiple variable comparison. $P < 0.05$ was considered as a significant difference.

3. Results

3.1. OVA induced mitochondrial dysfunction in airway epithelium of allergic asthma mice

In an OVA-induced allergic asthma mouse model, we observed significantly elevated RL and Cdyn, indicating increased airway hyperresponsiveness (Fig. 1A). H&E staining results confirmed the shedding of BECs, infiltration of inflammatory cells, smooth muscle proliferation, and thickening of alveolar septa in the lung tissue of the allergic asthma mouse model, validating successful model establishment (Fig. 1B-C). ELISA results demonstrated that OVA induction increased IL-4, IL-5, and IL-13 levels in the mouse lung tissue, suggesting elevated inflammation (Fig. 1D). OVA induction resulted in a decrease in ATP production and mtDNA copy number in mouse lung tissue (Fig. 1E-F). Furthermore, downregulation of TFAM accompanied by upregulation of PINK1 and OPTN were observed in allergic asthma mouse model lung tissues, suggesting mitophagy activation (Fig. 1G). The allergic asthma mouse model exhibited elevated ROS level, along with reduced SOD activity and GSH/GSSG ratio, as assessed by oxidative stress evaluation (Fig. 1H, S1A-B). These findings confirmed that OVA induced mitochondrial dysfunction in mouse lung tissue. Subsequently, in vitro experiments demonstrated that OVA induction significantly decreased the cell viability of BECs and caused mitochondrial swelling and deformation (Fig. 1I-J). Compared to the Control group, OVA-stimulated BECs showed decreased mitochondrial membrane potential, OCR, ATP levels, and mtDNA copy number, indicating mitochondrial dysfunction (Fig. 1K-N). WB analysis indicated that OVA induction led to a decrease in TFAM level and an increase in PINK1 and OPTN levels in the mitochondria of BECs, suggesting mitochondrial damage and mitophagy activation (Fig. 1O). Oxidative stress evaluation further validated that in OVA-stimulated BECs presented increased ROS and decreased antioxidant capacity (SOD, catalase activity, and GSH/GSSG ratio) (Fig. 1P, S1C-E). Collectively, these in vivo and in vitro research data provided compelling evidence that OVA induced mitochondrial dysfunction of airway epithelium.

3.2. GLCCI1 overexpression activated DYRK1A/FAM117B and KEAP1/NRF2 signaling pathways

Through qRT-PCR, WB, and IHC, we observed a significant reduction in both the mRNA and protein levels of GLCCI1 in the allergic asthma mouse model lung tissues (Fig. 2A-D, S4A). Bioinformatic analysis using the STRING database predicted a novel protein-protein interaction between GLCCI1 and DYRK1A (Fig. 2E), which we experimentally validated through Co-IP assays (Fig. 2F). Notably, OVA stimulation attenuated the interaction of DYRK1A and GLCCI1 in BECs (Fig. 2G). IF assays further demonstrated that OVA stimulation inhibited the expression and co-localization of DYRK1A and GLCCI1 (Fig. 2H). Moreover, both the mRNA and protein levels of DYRK1A and GLCCI1 were reduced in OVA-stimulated BECs (Fig. 2I-L). The results from qRT-PCR and IHC analyses corroborated that OVA induction led to a decrease in DYRK1A expression levels in mouse lung tissue (Fig. 2M-N, S4A). Thus, OVA treatment inhibited the expression and interaction of GLCCI1 and DYRK1A in the lung tissue of allergic asthma mouse models.

To further investigate the downstream signaling mechanism, we employed STRING database analysis which identified FAM117B as a novel DYRK1A-interacting partner (Fig. 3A). Co-IP assays validated the binding of DYRK1A to FAM117B, FAM117B to KEAP1, and KEAP1 to NRF2 (Figs. 3B-D). Following this, GLCCI1-OE were transfected to BECs (Fig. S3A-B). The results from IF assays indicated that GLCCI1-OE enhanced the expression and co-localization of DYRK1A and FAM117B, as well as FAM117B and KEAP1 in OVA-stimulated BECs (Fig. S2A-B). Additionally, GLCCI1-OE resulted in increased protein levels of GLCCI1, DYRK1A, p-DYRK1A, and FAM117B in these cells (Fig. 3E). qRT-PCR and WB confirmed that GLCCI1 overexpression did not alter NRF2 mRNA levels in OVA-stimulated BECs (Fig. 3F), while significantly elevating NRF2 protein level (Fig. 3G). To determine the mechanism by which GLCCI1 regulates NRF2 protein levels, OVA-stimulated cells were transfected with sh-GLCCI1 (Fig. S3C-D), followed by treatment with or without the proteasome inhibitor MG132. MG132 rescued the GLCCI1-knockdown-induced reduction of NRF2 (Fig. 3H). Cycloheximide chase assays further showed that GLCCI1 overexpression extended the half-life of NRF2 (Fig. 3I). Moreover, ubiquitination assays confirmed that GLCCI1 overexpression markedly reduced ubiquitination of NRF2 (Fig. 3J). These findings demonstrated that GLCCI1 suppressed ubiquitin-dependent degradation of NRF2. In summary, GLCCI1 regulated the DYRK1A/FAM117B and KEAP1/NRF2 signaling pathways in OVA-induced allergic asthma.

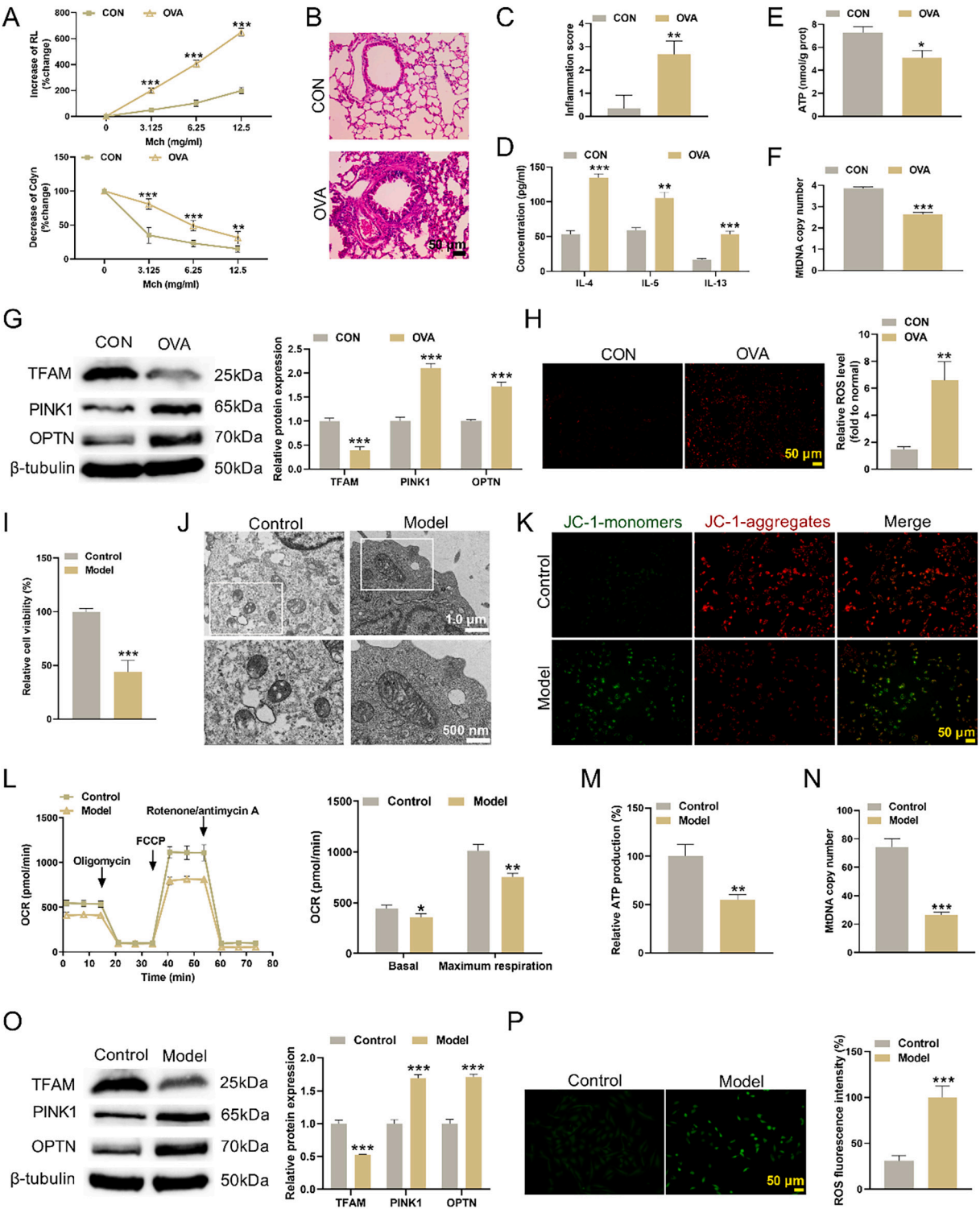

Fig. 1. OVA induction affected mitochondrial function of mouse airway epithelium. (A) RL and Cdyn of mice were measured 24 h after modeling to evaluate airway hyperresponsiveness. (B—C) The effects of OVA induction on mouse lung tissues were assessed using H&E staining. (D) The levels of IL-4, IL-5, and IL-13 were evaluated by ELISA detection. (E) An ATP assay kit was employed to measure ATP level in mouse lung tissues. (F) The mtDNA copy number in mouse lung tissue was evaluated through PCR detection. (G) WB was utilized to quantify the levels of TFAM, PINK1, and OPTN in the mitochondria. (H) ROS level in mouse lung tissue were assessed via a DHE assay. (I) The effect of OVA induction on the cell viability of BECs was evaluated using CCK-8 assay. (J) Electron microscopy was employed to observe the ultrastructure of BECs mitochondria. (K) The effect of OVA induction on the mitochondrial membrane potential of BECs was analyzed using a JC-1 mitochondrial membrane potential detection kit. (L-M) Kit detections were performed to evaluate the OCR and ATP levels of BECs. (N) The mtDNA copy number of BECs was measured through PCR detection. (O) WB detection was employed to quantify the expression levels of TFAM, PINK1, and OPTN in the mitochondria of BECs. (P) ROS level in BECs was measured using a ROS detection kit. $*p < 0.05$, $**p < 0.01$, $***p < 0.001$ vs CON/ Control. Data represent mean ± SD of three biological replicates, with each replicate containing three technical measurements.

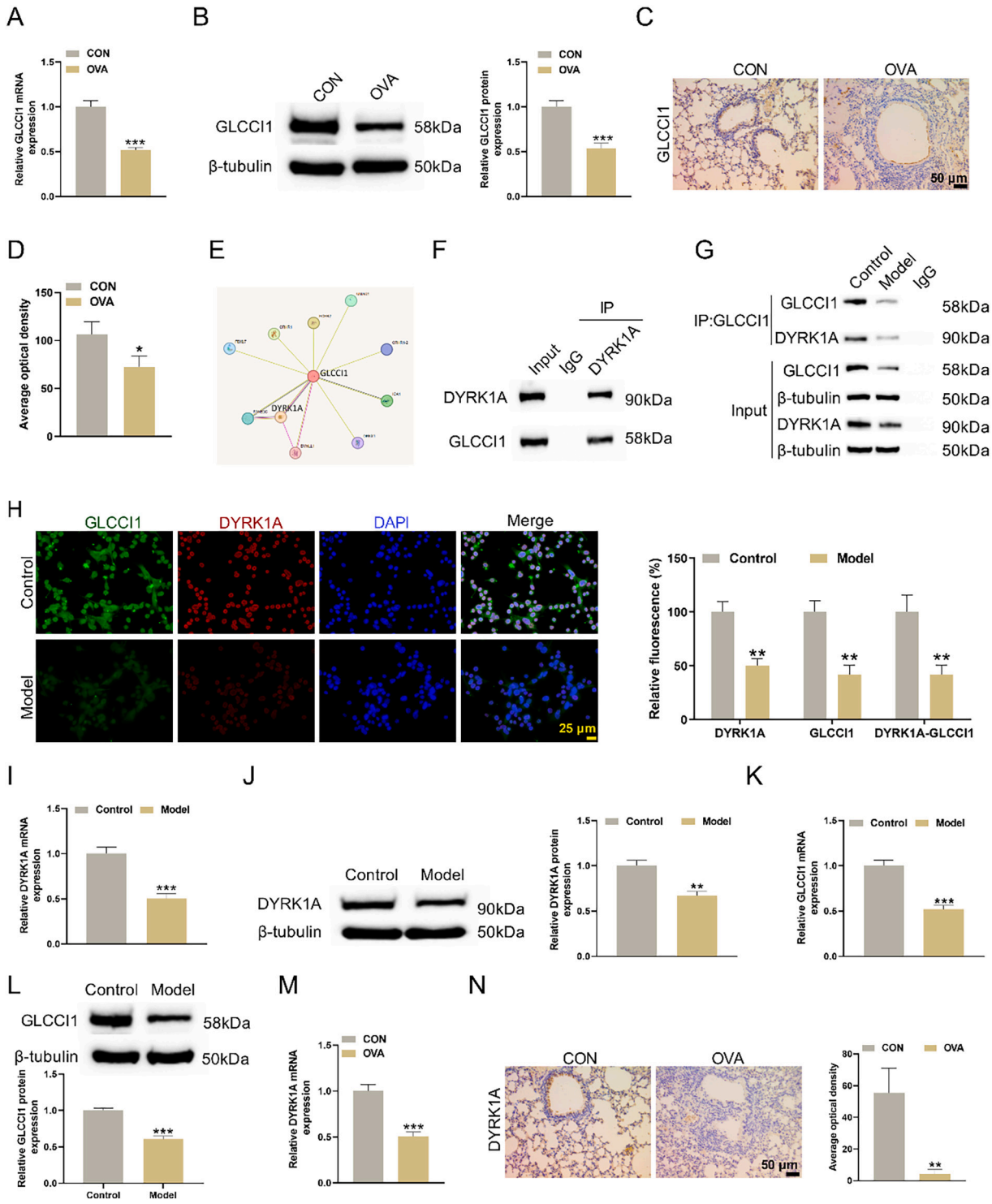

Fig. 2. OVA treatment influenced the expression and interaction of GLCCI1 and DYRK1A in lung tissue of allergic asthma mouse model. (A-D) The mRNA and protein levels of GLCCI1 in mouse lung tissue were evaluated using qRT-PCR, WB, and IHC. (E) To identify potential interacting proteins with GLCCI1, a screening was conducted utilizing the STRING database. (F-G) Co-IP assays were performed to confirm the interaction between DYRK1A and GLCCI1. (H) IF detection was employed to examine the expression and localization of DYRK1A and GLCCI1 in BECs. (I-L) qRT-PCR and WB were applied to assess the mRNA and protein levels of both DYRK1A and GLCCI1 in BECs. (M-N) The expression levels of DYRK1A in mouse lung tissue were measured through qRT-PCR and IHC detections. *p lt; 0.05, **$p < 0.01$, ***$p < 0.001$ vs CON/ Control. Data represent mean ± SD of three biological replicates, with each replicate containing three technical measurements.

3.3. GLCCI1 overexpression ameliorated mitochondrial dysfunction via the DYRK1A/FAM117B/NRF2 axis in OVA-stimulated BECs

WB and qRT-PCR showed that GLCCI1-OE significantly upregulated DYRK1A expression, while sh-DYRK1A did not significantly affect GLCCI1 level (Fig. 4A-B), confirming DYRK1A as a downstream effector of GLCCI1. GLCCI1 overexpression also increased mitochondrial membrane potential, OCR, mtDNA copy number and TFAM levels while decreasing PINK1 and OPTN levels in OVA-treated BECs, which were partly abolished by sh-DYRK1A (Fig. 4C-F).

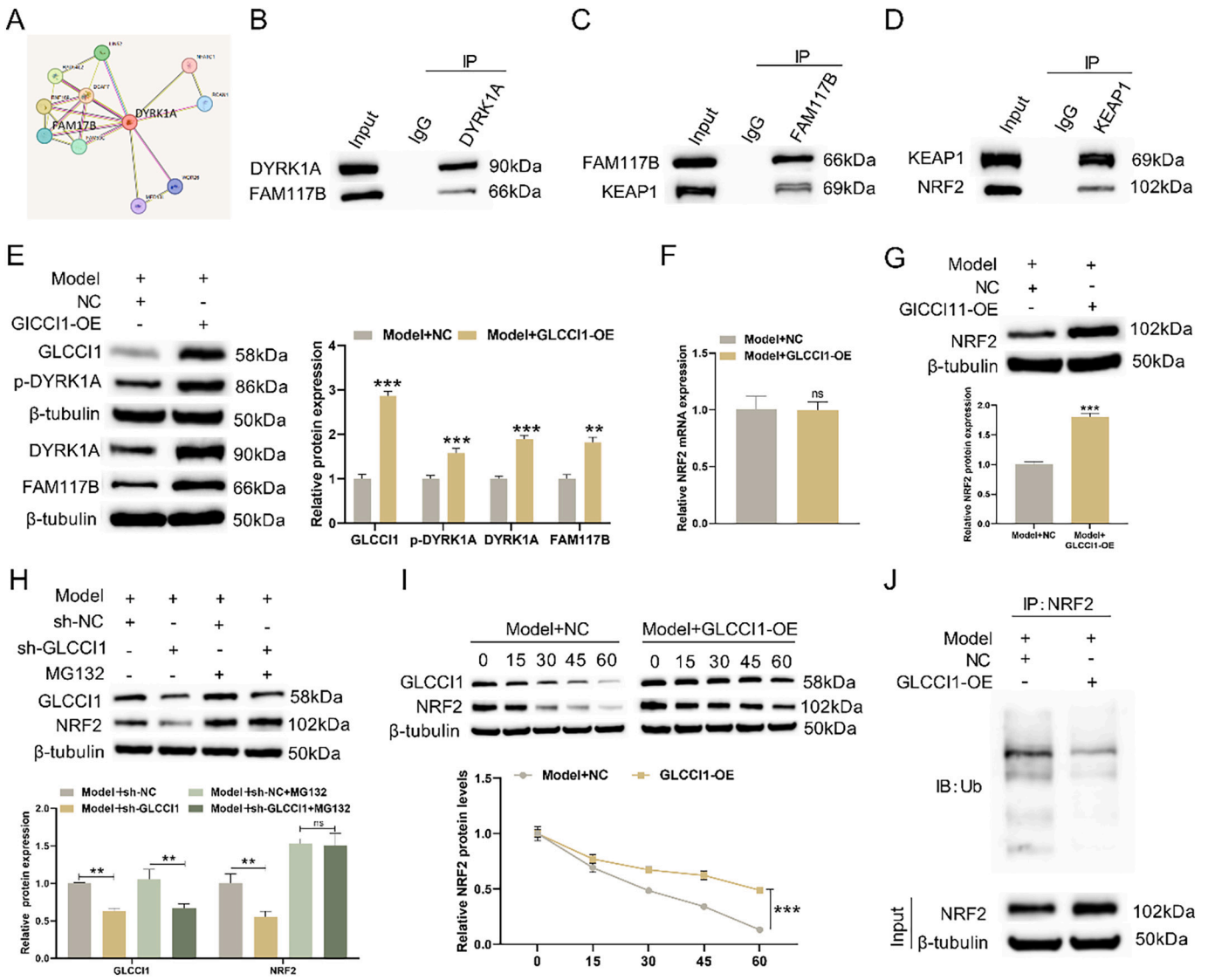

Fig. 3. Overexpression of GLCCI1 affected DYRK1A/FAM117B and KEAP1/NRF2 signaling pathways as well as NRF2 ubiquitination. (A) A screening of proteins that may interact with DYRK1A was conducted using the STRING database. (B—D) Co-IP assays were performed to confirm the interactions between DYRK1A and FAM117B, FAM117B and KEAP1, and KEAP1 and NRF2. (E) WB analysis was utilized to evaluate the effects of GLCCI1-OE on the protein expression levels of GLCCI1, DYRK1A, p-DYRK1A, and FAM117B. (F-G) qRT-PCR and WB were conducted to assess the effects of GLCCI1-OE on NRF2 mRNA and protein levels. (H) The effect of proteasome inhibitor MG132 on the reduction of NRF2 protein level by sh-GLCCI1 was assessed by WB. (I) Cycloheximide chase assay was performed to determine the impact of GLCCI1-OE on the degradation half-life of NRF2 protein. (J) The influence of GLCCI1-OE on NRF2 ubiquitination was observed by IP assay. $^{*}p < 0.05$, $^{**}p < 0.01$, $^{***}p < 0.001$ vs Model+NC/ Model+sh-NC/ Model+sh-NC + MG132. ns represents no significant difference. Data represent mean ± SD of three biological replicates, with each replicate containing three technical measurements.

To further elucidate the role of GLCCI1/DYRK1A/FAM117B in OVA-induced allergic asthma, sh-DYRK1A or sh-FAM117B were constructed, and their transfection efficiency in BECs was validated (Fig. S3E-H). WB confirmed that in OVA-stimulated BECs, sh-DYRK1A or sh-FAM117B attenuated the GLCCI1-OE-induced upregulation of NRF2 levels and the decrease in Cleaved PARP levels (Fig. 5A-B). Notably, in OVA-stimulated BECs with GLCCI1-OE, sh-DYRK1A resulted in a significant reduction in FAM117B levels, whereas sh-FAM117B did not significantly affect DYRK1A levels, indicating that FAM117B acted downstream of DYRK1A. In addition, IP assay revealed that sh-FAM117B or sh-DYRK1A counteracted the inhibition of NRF2 ubiquitination mediated by GLCCI1-OE (Fig. 5C). Functionally, in OVA-stimulated BECs, GLCCI1-OE led to the increase of ATP level, SOD activity, catalase activity, and GSH/GSSG ratio and the decrease of ROS level, which was reversed by sh-FAM117B or sh-DYRK1A (Fig. 5D-I). Results from the CCK-8 assay further revealed that sh-FAM117B or sh-DYRK1A impeded the GLCCI1-OE-induced restoration of cell viability in OVA-stimulated BECs (Fig. 5J). Collectively, these results demonstrated that GLCCI1 preserved mitochondrial function in allergic asthma through the DYRK1A/FAM117B/NRF2 pathway.

3.4. *GLCCI1 overexpression rescued mitochondrial function and attenuated airway remodeling in allergic asthma*

To investigate the role of GLCCI1 in regulating mitochondrial dysfunction in allergic asthma, BECs were transfected with GLCCI1-OE or sh-GLCCI1 prior to OVA treatment (Fig. S3A-D). qRT-PCR and WB analysis demonstrated that GLCCI1-OE resulted in a significant increase in GLCCI1 level, while sh-GLCCI1 led to a marked decrease in GLCCI1 level in OVA-treated BECs (Fig. 6A-B). Kit detections revealed that GLCCI1-OE elevated mitochondrial membrane potential, ATP, and OCR levels, whereas sh-GLCCI1 exhibited the opposite effects (Fig. 6C-F).

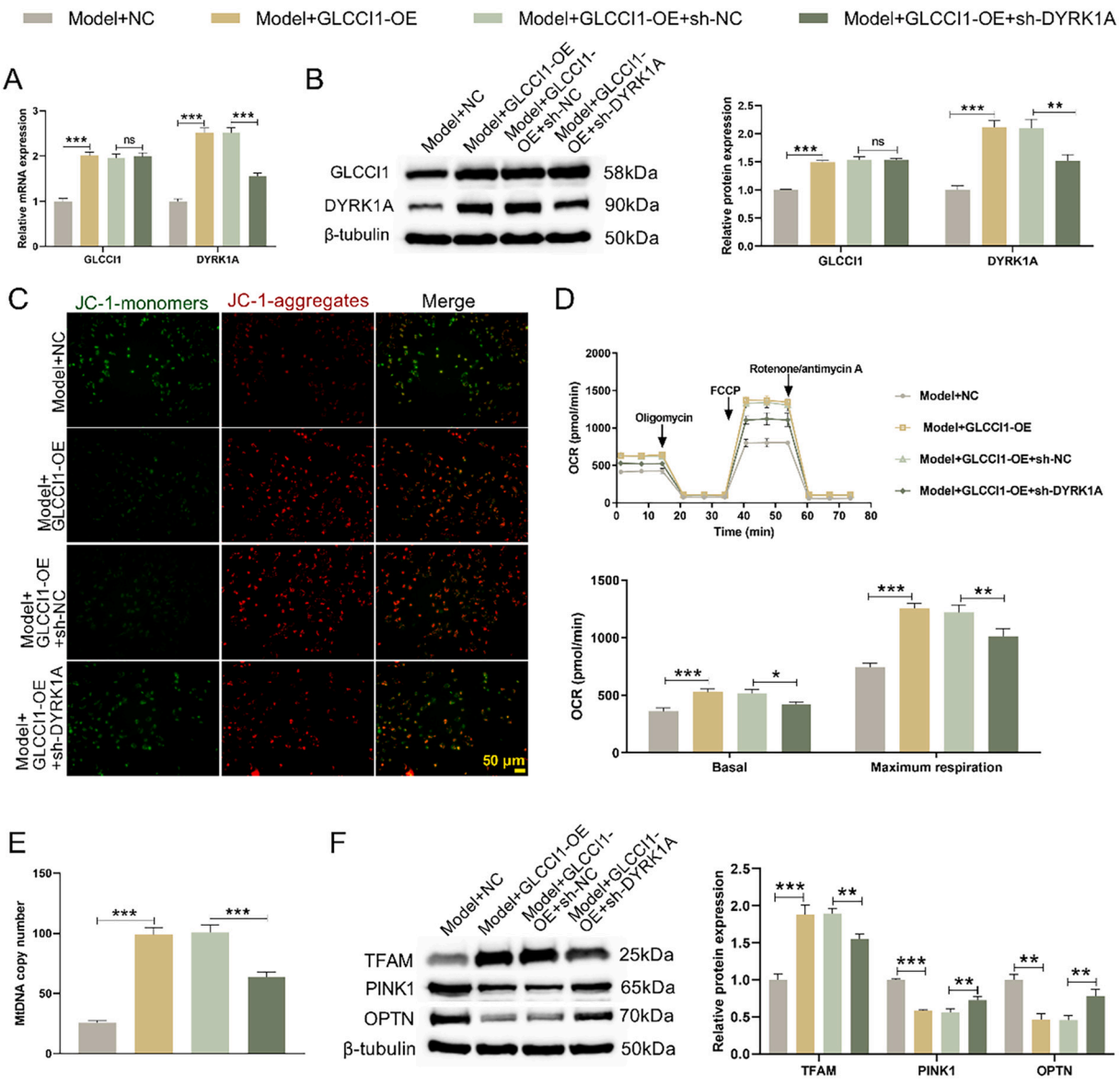

Fig. 4. GLCCI1 overexpression affected mitochondrial function via regulating DYRK1A. (A-B) qRT-PCR and WB analysis were employed to assess the levels of GLCCI1 and DYRK1A in BECs. (C) The JC-1 mitochondrial membrane potential detection kit was utilized to analyze the impact of GLCCI1-OE or GLCCI1-OE combined with sh-DYRK1A on the mitochondrial membrane potential of BECs. (D) The effects of GLCCI1-OE or GLCCI1-OE combined with sh-DYRK1A on the OCR level of BECs were assessed using a detection kit. (E) PCR assay was performed to measure the influence of GLCCI1-OE or GLCCI1-OE combined with sh-DYRK1A on mtDNA copy number in BECs. (F) WB detection was used to observe the expression levels of TFAM, PINK, and OPTN in the mitochondria of BECs. $^{*}p < 0.05$, $^{**}p < 0.01$, $^{***}p < 0.001$ vs Model+NC/ Model+GLCCI1-OE + sh-NC. Data represent mean ± SD of three biological replicates, with each replicate containing three technical measurements. (For interpretation of the references to colour in this figure legend, the reader is referred to the web version of this article.)

Moreover, GLCCI1-OE and sh-GLCCI1 showed opposite directions in regulating mtDNA copy number, TFAM, PINK1, OPTN level, ROS level, SOD activity, catalase activity, and GSH/GSSG ratio (Fig. 6G-N). The CCK-8 assay indicated that GLCCI1-OE significantly enhanced the viability of OVA-stimulated BECs, whereas sh-GLCCI1 reduced cell viability (Fig. 6O). Thus, GLCCI1 played a critical role in the regulation of mitochondrial dysfunction in OVA-stimulated BECs.

In allergic asthma mouse models, GLCCI1 overexpression resulted in increased levels of GLCCI1 mRNA and protein in lung tissues (Fig. 7A-B). IHC findings demonstrated that GLCCI1 overexpression caused upregulation of GLCCI1, DYRK1A, FAM117B and NRF2 in the lung tissue of allergic mice (Fig. 7C, S4B). Additionally, GLCCI1 overexpression led to elevated ATP level, mtDNA copy number, and TFAM level in lung tissue, while reducing the expression levels of PINK1 and OPTN (Fig. 7D-F). Results from kit detections indicated that overexpression of GLCCI1 also caused a decrease in ROS level, alongside an increase in SOD activity and GSH/GSSG ratio in lung tissue (Fig. 7G-I). H&E staining revealed that, compared to the OVA+LV-NC group, the lung tissues exhibited reduced shedding BECs, thinner alveolar septa, and decreased inflammatory cell infiltration in the OVA+LV-GLCCI1 group (Fig. 7J). ELISA results demonstrated that GLCCI1 overexpression markedly decreased IL-4, IL-5, and IL-13 levels in the lung tissue of allergic asthma mice, suggesting reduced inflammation (Fig. 7K). In addition, GLCCI1 overexpression caused the reduction of RL and Cdyn, demonstrating its potential to improve airway hyperresponsiveness in the allergic asthma mouse model (Fig. 7L). In consequence, GLCCI1 played a regulatory role in mitochondrial dysfunction and airway remodeling in allergic asthma mouse models.

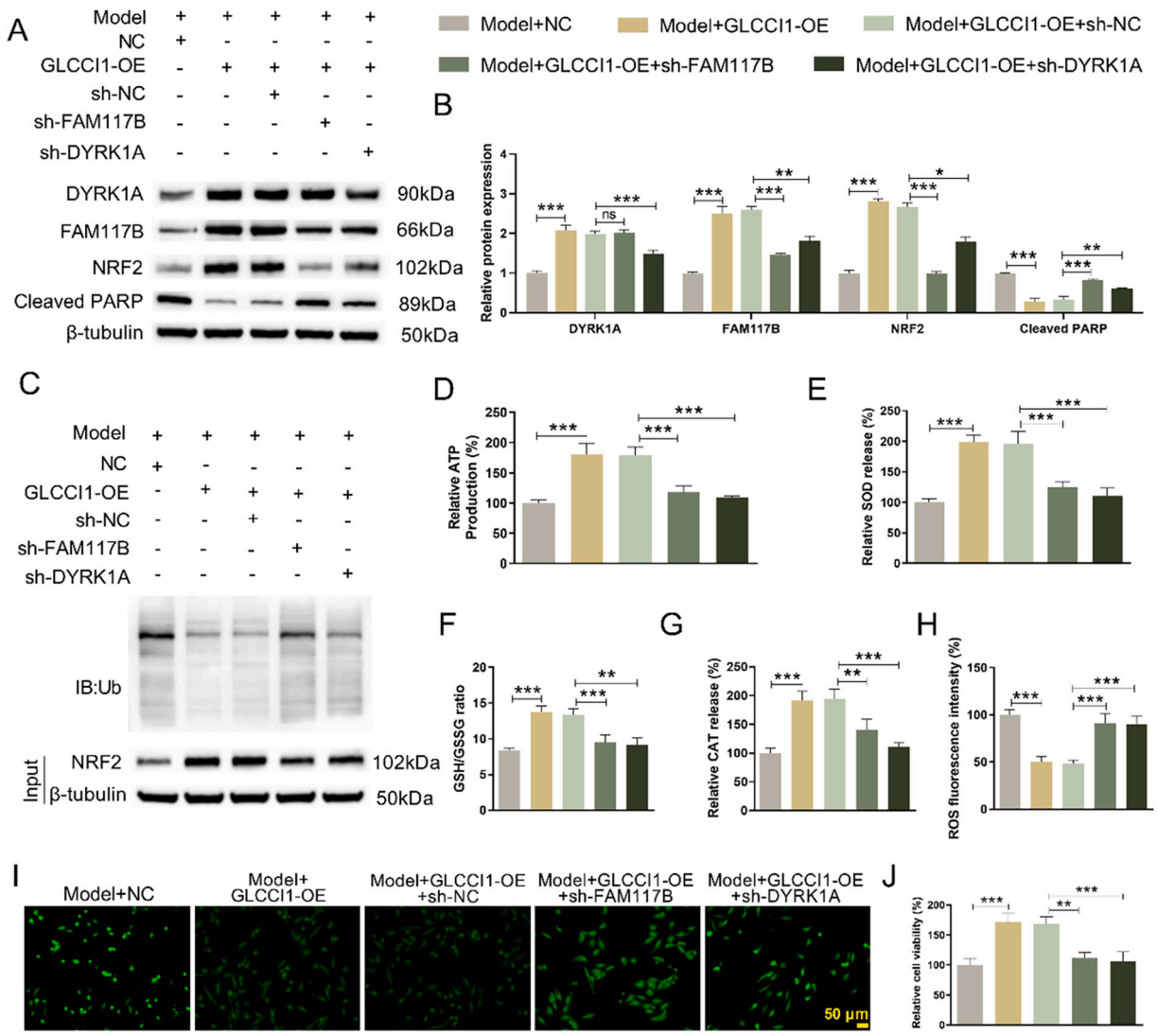

Fig. 5. GLCCI1 overexpression had influence on the mitochondrial function of BECs by modulating NRF2 ubiquitination through DYRK1A/FAM117B. (A-B) WB analysis was employed to assess the protein levels of DYRK1A, FAM117B, NRF2, and Cleaved PARP in BECs. (C) IP assay was conducted to investigate the regulation of sh-FAM117B or sh-DYRK1A on the inhibition of NRF2 ubiquitination by GLCCI1-OE. (D) The intracellular levels of ATP in BECs were measured using an ATP assay kit. (*E*-G) Kit assays were utilized to evaluate the activities of SOD and catalase, along with GSH/GSSG ratio within the mitochondria of BECs. (H—I) The intracellular levels of ROS in BECs were measured using ROS detection kit. (J) CCK-8 assay was performed to determine the impact of sh-FAM117B or sh-DYRK1A on regulating cell viability of BECs by GLCCI1-OE. *$p < 0.05$, **$p < 0.01$, ***$p < 0.001$ vs Model+NC/ Model+GLCCI1-OE + sh-NC. Data represent mean ± SD of three biological replicates, with each replicate containing three technical measurements.

4. Discussion

Allergic diseases are recognized by the World Health Organization as one of the three major health challenges that require prevention and control in the 21st century [23]. The high recurrence rate of allergic asthma causes significant suffering and imposes a substantial economic burden on patients [4]. Consequently, it is becoming increasingly important for physicians and scientists to elucidate the pathogenesis of allergic asthma. This study presented a novel molecular mechanism involving GLCCI1, which regulated mitochondrial function in allergic asthma. Specifically, GLCCI1 modulated mitochondrial dysfunction through DYRK1A/FAM117B/NRF2, thereby inhibiting the development of allergic asthma.

Mice represent an ideal model organism for studying allergic asthma owing to their well-defined immune system and genetic manipulability [24]. In our study, the OVA-induced allergic asthma mouse model recapitulated key clinical features, including pronounced airway hyperresponsiveness [25], and characteristic pathological alterations in the bronchial epithelium. As the primary barrier against environmental insults, the airway epithelium undergoes significant structural and functional impairments in asthma, manifesting as epithelial shedding, barrier dysfunction, and pronounced inflammatory infiltration [26,27]. Our experimental model successfully reproduced these hallmark features, confirming its validity for mechanistic investigations. Importantly, research highlights the central role of BEC mitochondria in asthma pathogenesis, with mitochondrial dysfunction being regulated through complex cellular signaling networks [28,29]. Mitochondrial dysfunction in allergic asthma is characterized by alterations in mitochondrial membrane potential, ATP level, ROS level, mtDNA copy number, TFAM, and PINK1 [29]. This study confirmed that OVA induction led to a decrease in mitochondrial membrane potential, ATP level, mtDNA copy number and TFAM, alongside an increase in ROS level and PINK1 in BECs. Notably, GLCCI1-OE and sh-GLCCI1 exhibited opposing effects on these mitochondrial function indicators. Additionally, GLCCI1-OE demonstrated a beneficial impact on the recovery of mitochondrial function. Therefore, GLCCI1 appeared to ameliorate

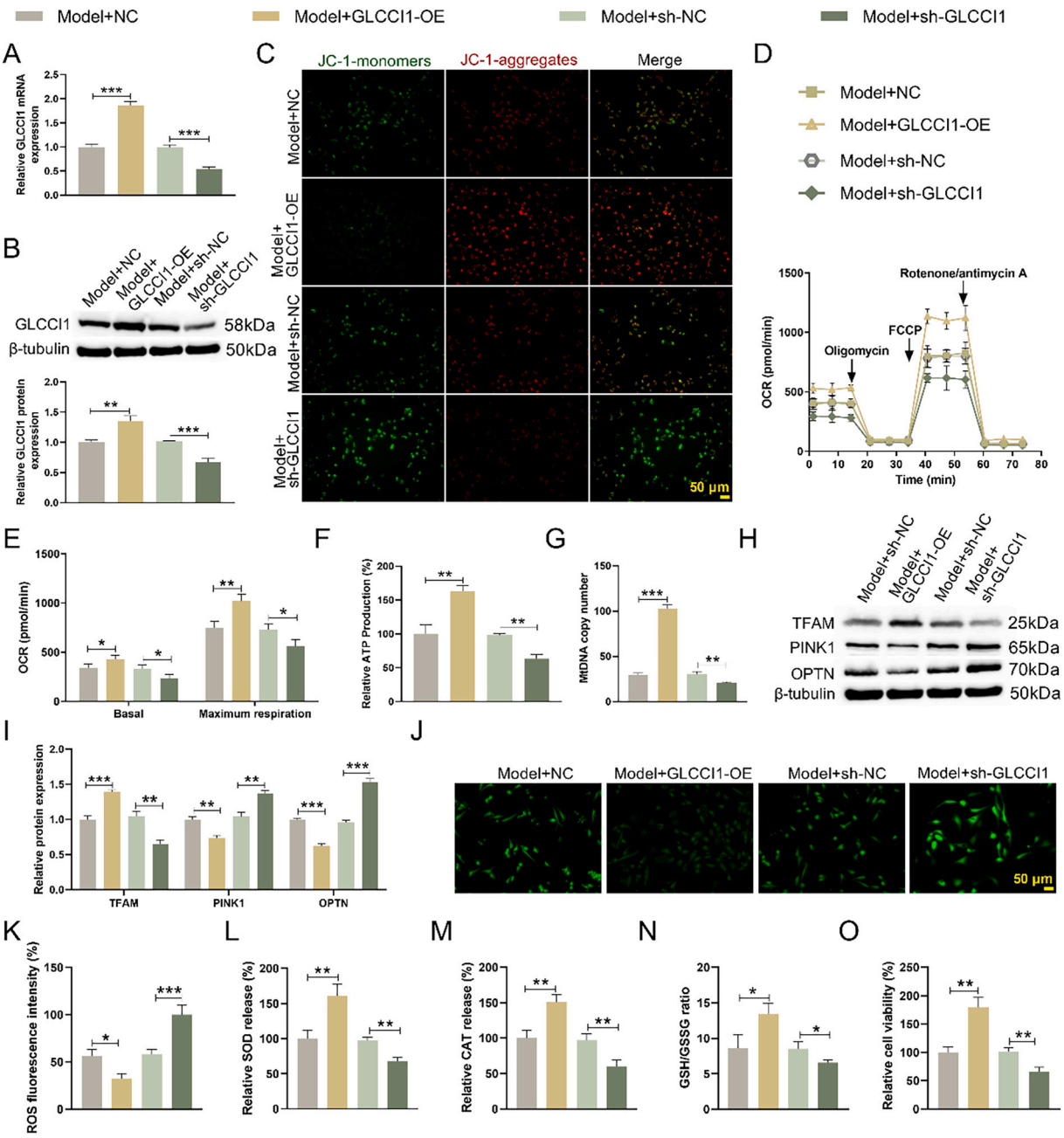

Fig. 6. GLCCI1 regulated mitochondrial dysfunction in OVA-stimulated BECs. (A-B) qRT-PCR and WB analyses were conducted to evaluate the expression levels of GLCCI1 in OVA-stimulated BECs. (C) The impact of GLCCI1-OE or sh-GLCCI1 on mitochondrial membrane potential was assessed using the JC-1 mitochondrial membrane potential detection kit. (D—F) The kit assay was employed to evaluate the effects of GLCCI1-OE or sh-GLCCI1 on OCR and ATP levels in OVA-stimulated BECs. (G) The influence of GLCCI1-OE or sh-GLCCI1 on mtDNA copy number in OVA-stimulated BECs was analyzed through PCR detection. (H—I) WB analysis was performed to measure the expression levels of TFAM, PINK1, and OPTN in OVA-stimulated BECs. (J-N) The effects of GLCCI1-OE or sh-GLCCI1 on ROS levels, SOD activity, catalase activity, and GSH/GSSG ratio were evaluated using the kit assays. (O) CCK-8 assay was utilized to observe the effects of GLCCI1-OE or sh-GLCCI1 on the cell viability of OVA-stimulated BECs. *$p < 0.05$, **$p < 0.01$, ***$p < 0.001$ vs Model+NC/ Model+sh-NC. Data represent mean ± SD of three biological replicates, with each replicate containing three technical measurements.

mitochondrial dysfunction in the lung tissue of allergic asthmatic mice.

In various disease contexts, the activation of the KEAP1/NRF2 signaling pathway has been shown to improve mitochondrial dysfunction [12,30,31]. Besides, sesamin has been found to increase NRF2 levels and reduce airway inflammation in asthma by modulating mitophagy and mitochondrial apoptosis [32]. Research conducted by Ravindra demonstrates that artesunate significantly elevates NRF2 levels and activates the KEAP1/NRF2 pathway, contributing to the alleviation of allergic asthma [33]. However, there remains a gap in the investigation of the upstream regulatory mechanisms governing the KEAP1/NRF2 signaling pathway specifically in the context of allergic asthma. Moreover, GLCCI1 and FAM117B have been identified as interacting proteins of DYRK1A [34]. Utilizing the STRING database [20,21] and Co-IP detection, we further demonstrated the binding interactions between DYRK1A and FAM117B, FAM117B and KEAP1, as well as KEAP1 and NRF2. Moreover, this study confirmed that GLCCI1 overexpression activated the NRF2 signaling pathway and ameliorated mitochondrial dysfunction by promoting DYRK1A/FAM117B. These findings are consistent with previously reported roles of DYRK1A and FAM117B in activating the NRF2 signaling pathway in other disease models [18,19].

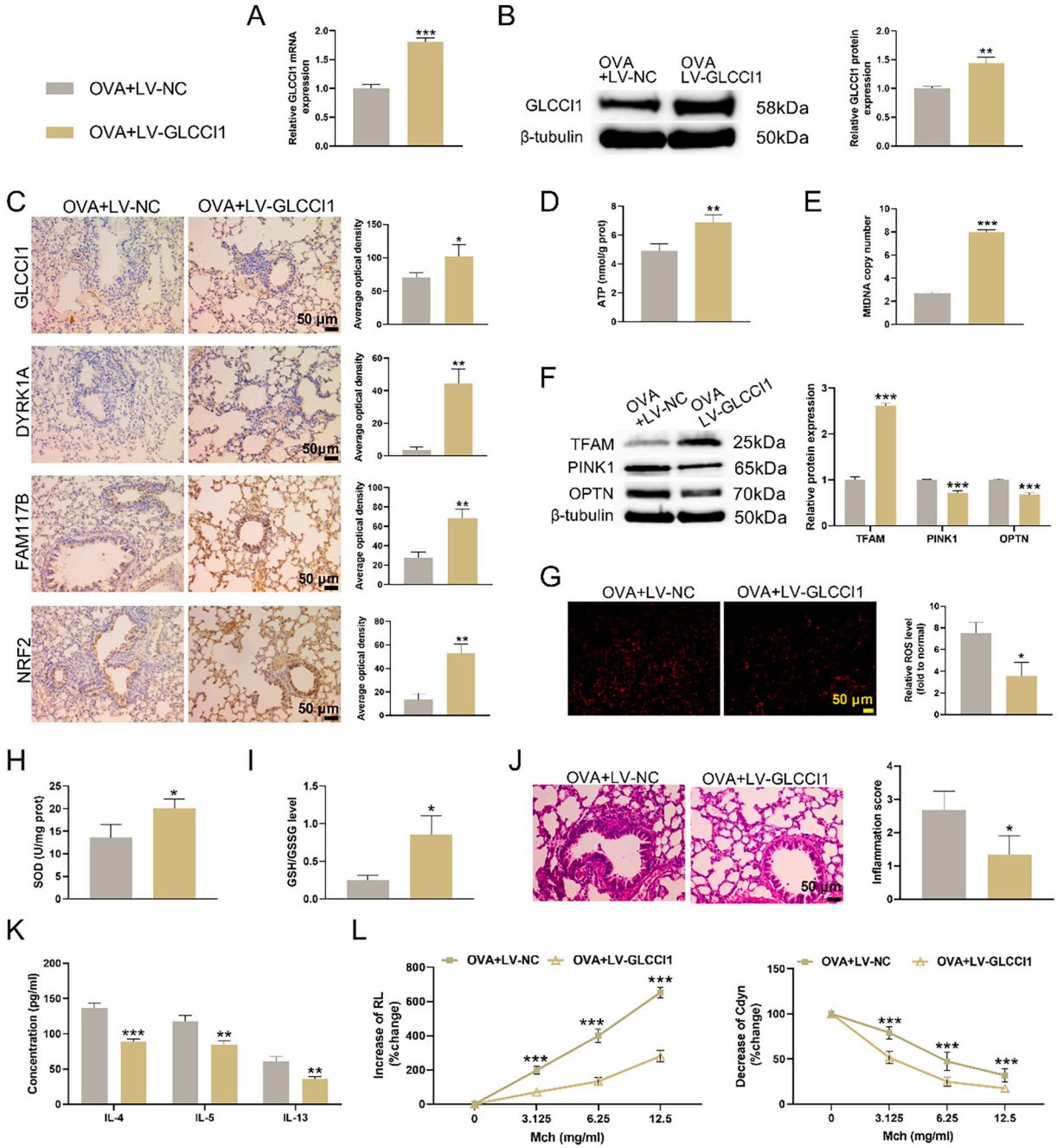

Fig. 7. Overexpression of GLCCI1 influenced mitochondrial function and airway remodeling in allergic asthma mouse models. (A-B) qRT-PCR and WB analyses were conducted to assess the impact of LV-GLCCI1 on GLCCI1 expression levels in the lung tissue of allergic asthma mouse models. (C) The effect of LV-GLCCI1 on the expression of GLCCI1, DYRK1A, FAM117B and NRF2 in allergic asthma mice was observed by IHC assay. (D) A kit assay was employed to evaluate the effect of LV-GLCCI1 on ATP levels in the lung tissue. (E) PCR detection was utilized to analyze the influence of LV-GLCCI1 on mtDNA copy number in the lung tissue. (F) WB analysis was performed to measure the expression levels of TFAM, PINK1, and OPTN in the mitochondria of lung tissue. (G-I) The effects of LV-GLCCI1 on ROS levels, SOD activity, and GSH/GSSG ratio in lung tissue were assessed using kit detection methods. (J) H&E staining was applied to observe the pathological changes in lung tissue resulting from LV-GLCCI1 treatment in allergic asthma mouse models. (K) The levels of IL-4, IL-5, and IL-13 were evaluated by ELISA detection. (L) RL and Cdyn were measured 24 h post-modeling to evaluate the impact of LV-GLCCI1 on airway hyperresponsiveness in allergic asthma mouse models. $^{*}p < 0.05$, $^{**}p < 0.01$, $^{***}p < 0.001$ vs OVA+LV-NC. Data represent mean ± SD of three biological replicates, with each replicate containing three technical measurements.

Notably, our study represents the first elucidation of the molecular mechanism by which GLCCI1 regulates the NRF2 signaling pathway in allergic asthma.

In diabetic nephropathy models, NRF2 activation has been shown to ameliorate renal tubular injury by upregulating PINK1-mediated autophagy [35]. In contrast, our allergic asthma model demonstrated suppressed NRF2 signaling alongside elevated levels of autophagy-related proteins PINK1 and OPTN. These findings are consistent with established literature showing NRF2 downregulation in OVA-induced asthma [36] and PINK1 upregulation during allergic airway inflammation [37,38]. These opposing patterns suggest allergic inflammation may involve impaired NRF2 signaling coupled with compensatory mitophagy activation. Future studies should investigate the precise relationship between NRF2 signaling and mitophagy in allergic asthma to determine whether NRF2 suppression creates permissive conditions for aberrant mitophagy activation, which would significantly advance

our understanding of NRF2's multifaceted roles in maintaining bronchial epithelial mitochondrial homeostasis during inflammatory diseases.

This study provided new insights into the pathogenesis of allergic asthma and novel therapeutic targets aimed at improving mitochondrial function. However, several critical questions remain unresolved. The research utilized OVA-induced allergic asthma mice to simulate mitochondrial conditions during disease onset. The mitochondrial dysfunction is known to influence asthma severity [29]. The conclusions of this study will require further validation in varying severities mouse models and different species models to ascertain their scientific and clinical significance. Additionally, studies demonstrate that the kinase DYRK1A regulates mitochondrial structure and function by phosphorylating TOM70, thereby modulating its interaction with the TOM core complex [39,40]. have NRF2's critical role in promoting mitochondrial biogenesis has been established [41,42], while reduced mitochondrial oxidative stress has been shown to influence TOM70 expression [43]. Notably, recent work reveals that cepharanthine disrupts mitochondrial function by inhibiting TOM70, consequently suppressing NRF2-driven ferroptosis in colorectal cancer cells [44]. Future investigations elucidating how DYRK1A-dependent NRF2 activation potentially affects mitochondrial proteins (including TOM70) could provide deeper mechanistic insights and therapeutic opportunities for allergic asthma.

5. Conclusion

This study utilized animal and cell models to elucidate the specific mechanisms by which GLCCI1 regulated mitochondrial dysfunction in allergic asthma. Specifically, GLCCI1 overexpression activated NRF2 signaling pathway via DYRK1A/FAM117B, thereby restoring mitochondrial function of allergic asthma mice. While the conclusions drawn from this study warrant further validation across a broader range of allergic asthma models, the findings offered valuable insights into the pathogenesis of allergic asthma and highlight potential new therapeutic targets.

CRediT authorship contribution statement

Qiufen Xun: Supervision, Resources, Project administration, Investigation, Formal analysis, Data curation, Conceptualization. **Qing Yang:** Writing – review & editing, Writing – original draft, Formal analysis, Data curation, Conceptualization. **Wei Wang:** Writing – review & editing, Methodology, Formal analysis. **Guofeng Zhu:** Writing – review & editing, Validation, Software.

Consent for publication

Not applicable.

Ethics approval

All animal experiments were conducted with the approval of the Experimental Animal Ethics Committee of Second Affiliated Hospital of Nanchang University.

Funding

This work was supported by Natural Science Foundation of Jiangxi Province (No. 20212BAB216046), Science and Technology Project of Education Department of Jiangxi Province (No. GJJ200195) and the National Natural Science Foundation of China (No. 81860006).

Declaration of competing interest

The authors declare no competing interests.

Appendix A. Supplementary data

Supplementary data to this article can be found online at https://doi.org/10.1016/j.cellsig.2025.111929.

Data availability

All data generated and/or analyzed during the current study are available from the corresponding author on reasonable request.

References

[1] N.G. Papadopoulos, M. Miligkos, P. Xepapadaki, A current perspective of allergic asthma: from mechanisms to management, Handb. Exp. Pharmacol. 268 (2022) 69–93.
[2] M. Schatz, L. Rosenwasser, The allergic asthma phenotype, J Allergy Clin Immunol Pract 2 (6) (2014), 645–8; quiz 649.
[3] N. Akar-Ghibril, T. Casale, A. Custovic, W. Phipatanakul, Allergic endotypes and phenotypes of asthma, J Allergy Clin Immunol Pract 8 (2) (2020) 429–440.
[4] J. Wang, Y. Zhou, H. Zhang, L. Hu, J. Liu, L. Wang, T. Wang, H. Zhang, L. Cong, Q. Wang, Pathogenesis of allergic diseases and implications for therapeutic interventions, Signal Transduct. Target. Ther. 8 (1) (2023) 138.
[5] D. Iyer, N. Mishra, A. Agrawal, Mitochondrial function in allergic disease, Curr Allergy Asthma Rep 17 (5) (2017) 29.
[6] P.H. Reddy, Mitochondrial dysfunction and oxidative stress in asthma: implications for mitochondria-targeted antioxidant therapeutics, Pharmaceuticals (Basel) 4 (3) (2011) 429–456.
[7] D. Gras, P. Chanez, I. Vachier, A. Petit, A. Bourdin, Bronchial epithelium as a target for innovative treatments in asthma, Pharmacol. Ther. 140 (3) (2013) 290–305.
[8] J.H. Kang, S.M. Hwang, I.Y. Chung, S100A8, S100A9 and S100A12 activate airway epithelial cells to produce MUC5AC via extracellular signal-regulated kinase and nuclear factor-κB pathways, Immunology 144 (1) (2015) 79–90.
[9] U. Mabalirajan, J. Aich, G.D. Leishangthem, S.K. Sharma, A.K. Dinda, B. Ghosh, Effects of vitamin E on mitochondrial dysfunction and asthma features in an experimental allergic murine model, J. Appl. Physiol. 107 (4) (2009) 1285–1292 (1985).
[10] J. Ariza, J.A. González-Reyes, L. Jódar, A. Díaz-Ruiz, R. de Cabo, J.M. Villalba, Mitochondrial permeabilization without caspase activation mediates the increase of basal apoptosis in cells lacking Nrf2, Free Radic. Biol. Med. 95 (2016) 82–95.
[11] H. Shan, X. Li, C. Ouyang, H. Ke, X. Yu, J. Tan, J. Chen, C. Wang, L. Zhang, Y. Tang, L. Yu, W. Li, Salidroside prevents PM2.5-induced BEAS-2B cell apoptosis via SIRT1-dependent regulation of ROS and mitochondrial function, Ecotoxicol. Environ. Saf. 231 (2022) 113170.
[12] X. Luo, Y. Wang, X. Zhu, Y. Chen, B. Xu, X. Bai, X. Weng, J. Xu, Y. Tao, D. Yang, J. Du, Y. Lv, S. Zhang, S. Hu, J. Li, H. Jia, MCL attenuates atherosclerosis by suppressing macrophage ferroptosis via targeting KEAP1/NRF2 interaction, Redox Biol. 69 (2024) 102987.
[13] Z. Kiuchi, Y. Nishibori, S. Kutsuna, M. Kotani, I. Hada, T. Kimura, T. Fukutomi, D. Fukuhara, N. Ito-Nitta, A. Kudo, T. Takata, Y. Ishigaki, N. Tomosugi, H. Tanaka, S. Matsushima, S. Ogasawara, Y. Hirayama, H. Takematsu, K. Yan, GLCCI1 is a novel protector against glucocorticoid-induced apoptosis in T cells, FASEB J. 33 (6) (2019) 7387–7402.
[14] K. Hirai, T. Shirai, Y. Rachi, S. Uehara, M. Ueda, E. Nakatani, K. Itoh, Impact of gene expression associated with glucocorticoid-induced transcript 1 (GLCCI1) on severe asthma and future exacerbation, Biol. Pharm. Bull. 42 (10) (2019) 1746–1752.
[15] Q. Xun, J. Kuang, Q. Yang, W. Wang, G. Zhu, GLCCI1 reduces collagen deposition and airway hyper-responsiveness in a mouse asthma model through binding with WD repeat domain 45B, J. Cell. Mol. Med. 25 (14) (2021) 6573–6583.
[16] J. Liu, H. Yu, S. Yu, M. Liu, X. Chen, Y. Wang, J. Li, C. Shi, W. Liu, Z. Zuo, X. Liu, GLCCI1 alleviates GRP78-initiated endoplasmic reticulum stress-induced apoptosis of retinal ganglion cells in diabetic retinopathy by upregulating and interacting with HSP90AB1, Sci. Rep. 14 (1) (2024) 26665.
[17] J. Hwang, A. Park, C. Kim, D. Yu, H. Byun, M. Ku, J. Yang, T.I. Kim, K.S. Jeong, K. Y. Kim, H. Lee, S.J. Shin, Suppression of DYRK1A/B drives endoplasmic reticulum stress-mediated autophagic cell death through metabolic reprogramming in colorectal Cancer cells, Anticancer Res. 42 (1) (2022) 589–598.
[18] C. Noll, A. Tlili, C. Ripoll, L. Mallet, J.L. Paul, J.M. Delabar, N. Janel, Dyrk1a activates antioxidant NQO1 expression through an ERK1/2-Nrf2 dependent mechanism, Mol. Genet. Metab. 105 (3) (2012) 484–488.
[19] Y. Zhou, Y. Chen, Y. Shi, L. Wu, Y. Tan, T. Li, Y. Chen, J. Xia, R. Hu, FAM117B promotes gastric cancer growth and drug resistance by targeting the KEAP1/NRF2 signaling pathway, J. Clin. Invest. 133 (3) (2023).
[20] V.R. Menon, V. Ananthapadmanabhan, S. Swanson, S. Saini, F. Sesay, V. Yakovlev, L. Florens, J.A. DeCaprio, M.P. Washburn, M. Dozmorov, L. Litovchick, DYRK1A regulates the recruitment of 53BP1 to the sites of DNA damage in part through interaction with RNF169, Cell Cycle 18 (5) (2019) 531–551.
[21] E.L. Huttlin, R.J. Bruckner, J. Navarrete-Perea, J.R. Cannon, K. Baltier, F. Gebreab, M.P. Gygi, A. Thornock, G. Zarraga, S. Tam, J. Szpyt, B.M. Gassaway, A. Panov, H. Parzen, S. Fu, A. Golbazi, E. Maenpaa, K. Stricker, S. Guha Thakurta, T. Zhang, R. Rad, J. Pan, D.P. Nusinow, J.A. Paulo, D.K. Schweppe, L.P. Vaites, J.W. Harper,

S.P. Gygi, Dual proteome-scale networks reveal cell-specific remodeling of the human interactome, Cell 184 (11) (2021) 3022–3040.e28.
[22] J.P. Rooney, I.T. Ryde, L.H. Sanders, E.H. Howlett, M.D. Colton, K.E. Germ, G. D. Mayer, J.T. Greenamyre, J.N. Meyer, PCR based determination of mitochondrial DNA copy number in multiple species, Methods Mol. Biol. 1241 (2015) 23–38.
[23] J. Bousquet, P. Van Cauwenberge, N. Khaltaev, Allergic rhinitis and its impact on asthma, J. Allergy Clin. Immunol. 108 (5 Suppl) (2001) S147–S334.
[24] J.C. Kips, G.P. Anderson, J.J. Fredberg, U. Herz, M.D. Inman, M. Jordana, D. M. Kemeny, J. Lötvall, R.A. Pauwels, C.G. Plopper, D. Schmidt, P.J. Sterk, A.J. Van Oosterhout, B.B. Vargaftig, K.F. Chung, Murine models of asthma, Eur. Respir. J. 22 (2) (2003) 374–382.
[25] M. Casaro, V.R. Souza, F.A. Oliveira, C.M. Ferreira, OVA-induced allergic airway inflammation mouse model, Methods Mol. Biol. 2019 (1916) 297–301.
[26] P.W. Hellings, B. Steelant, Epithelial barriers in allergy and asthma, J. Allergy Clin. Immunol. 145 (6) (2020) 1499–1509.
[27] Z.I. Komlósi, W. van de Veen, N. Kovács, G. Szűcs, M. Sokolowska, L. O'Mahony, M. Akdis, C.A. Akdis, Cellular and molecular mechanisms of allergic asthma, Mol. Asp. Med. 85 (2022) 100995.
[28] D.J. Rowlands, Mitochondria dysfunction: a novel therapeutic target in pathological lung remodeling or bystander? Pharmacol. Ther. 166 (2016) 96–105.
[29] L. Qian, E. Mehrabi Nasab, S.M. Athari, S.S. Athari, Mitochondria signaling pathways in allergic asthma, J. Investig. Med. 70 (4) (2022) 863–882.
[30] X. Lan, Q. Wang, Y. Liu, Q. You, W. Wei, C. Zhu, D. Hai, Z. Cai, J. Yu, J. Zhang, N. Liu, Isoliquiritigenin alleviates cerebral ischemia-reperfusion injury by reducing oxidative stress and ameliorating mitochondrial dysfunction via activating the Nrf2 pathway, Redox Biol. 77 (2024) 103406.
[31] A.A. Bhat, E. Moglad, A. Goyal, M. Afzal, R. Thapa, W.H. Almalki, I. Kazmi, S. I. Alzarea, H. Ali, A. Gaur, T.G. Singh, S.K. Singh, K. Dua, G. Gupta, Nrf2 pathways in neuroprotection: alleviating mitochondrial dysfunction and cognitive impairment in aging, Life Sci. 357 (2024) 123056.
[32] Q. Bai, Z. Wang, Y. Piao, X. Zhou, Q. Piao, J. Jiang, H. Liu, H. Piao, L. Li, Y. Song, G. Yan, Sesamin alleviates asthma airway inflammation by regulating mitophagy and mitochondrial apoptosis, J. Agric. Food Chem. 70 (16) (2022) 4921–4933.
[33] K.C. Ravindra, W.E. Ho, C. Cheng, L.C. Godoy, J.S. Wishnok, C.N. Ong, W.S. Wong, G.N. Wogan, S.R. Tannenbaum, Untargeted proteomics and systems-based mechanistic investigation of artesunate in human bronchial epithelial cells, Chem. Res. Toxicol. 28 (10) (2015) 1903–1913.
[34] V. Ananthapadmanabhan, K.H. Shows, A.J. Dickinson, L. Litovchick, Insights from the protein interaction universe of the multifunctional "goldilocks" kinase DYRK1A, Front. Cell Dev. Biol. 11 (2023) 1277537.
[35] L. Xiao, X. Xu, F. Zhang, M. Wang, Y. Xu, D. Tang, J. Wang, Y. Qin, Y. Liu, C. Tang, L. He, A. Greka, Z. Zhou, F. Liu, Z. Dong, L. Sun, The mitochondria-targeted antioxidant MitoQ ameliorated tubular injury mediated by mitophagy in diabetic kidney disease via Nrf2/PINK1, Redox Biol. 11 (2017) 297–311.
[36] D. Bai, T. Sun, F. Lu, Y. Shen, Y. Zhang, B. Zhang, G. Yu, H. Li, J. Hao, Eupatilin suppresses OVA-induced asthma by inhibiting NF-κB and MAPK and activating Nrf2 Signaling pathways in mice, Int. J. Mol. Sci. 23 (3) (2022).
[37] S. Liu, C. Wang, Y. Zhang, Y. Zhang, Y. Song, J. Jiang, R. Liu, H. Jin, G. Yan, Y. Jin, Polydatin inhibits mitochondrial damage and mitochondrial ROS by promoting PINK1-parkin-mediated mitophagy in allergic rhinitis, FASEB J. 37 (4) (2023) e22852.
[38] H. Ding, X. Lu, H. Wang, W. Chen, B. Niu, NLRP3 inflammasome deficiency alleviates inflammation and oxidative stress by promoting PINK1/parkin-mediated mitophagy in allergic rhinitis mice and nasal epithelial cells, J. Asthma Allergy 17 (2024) 717–731.
[39] C. Walter, A. Marada, T. Suhm, R. Ernsberger, V. Muders, C. Kücükköse, P. Sánchez-Martín, Z. Hu, A. Aich, S. Loroch, F.A. Solari, D. Poveda-Huertes, A. Schwierzok, H. Pommerening, S. Matic, J. Brix, A. Sickmann, C. Kraft, J. Dengjel, S. Dennerlein, T. Brummer, F.N. Vögtle, C. Meisinger, Global kinome profiling reveals DYRK1A as critical activator of the human mitochondrial import machinery, Nat. Commun. 12 (1) (2021) 4284.
[40] A. Marada, C. Walter, T. Suhm, S. Shankar, A. Nandy, T. Brummer, I. Dhaouadi, F. N. Vögtle, C. Meisinger, DYRK1A signalling synchronizes the mitochondrial import pathways for metabolic rewiring, Nat. Commun. 15 (1) (2024) 5265.
[41] Q.M. Chen, Nrf2 for protection against oxidant generation and mitochondrial damage in cardiac injury, Free Radic. Biol. Med. 179 (2022) 133–143.
[42] M. George, M. Tharakan, J. Culberson, A.P. Reddy, P.H. Reddy, Role of Nrf2 in aging, Alzheimer's and other neurodegenerative diseases, Ageing Res. Rev. 82 (2022) 101756.
[43] H.F. Pei, J.N. Hou, F.P. Wei, Q. Xue, F. Zhang, C.F. Peng, Y. Yang, Y. Tian, J. Feng, J. Du, L. He, X.C. Li, E.H. Gao, D. Li, Y.J. Yang, Melatonin attenuates postmyocardial infarction injury via increasing Tom70 expression, J. Pineal Res. 62 (1) (2017).
[44] L.G. Li, D. Zhang, Q. Huang, M. Yan, N.N. Chen, Y. Yang, R.C. Xiao, H. Liu, N. Han, A.M. Qureshi, J. Hu, F. Leng, Y.J. Hui, Mitochondrial disruption resulting from Cepharanthine-mediated TOM inhibition triggers ferroptosis in colorectal cancer cells, J. Cancer Res. Clin. Oncol. 150 (10) (2024) 460.